

## STABILITY OF SEA-SALT DELIQUESCENT BRINES ON HEATED SURFACES OF SNF DRY STORAGE CANISTERS

Charles Bryan<sup>1</sup>, Eric Schindelholz, Andrew Knight, Jason Taylor, Remi Dingreville

*Sandia National Laboratories, P.O. Box 5800, Albuquerque, NM 87185, <sup>1</sup>crbryan@sandia.gov*

*For long-term storage, spent nuclear fuel (SNF) is placed in dry storage systems, commonly consisting of welded stainless steel canisters enclosed in ventilated overpacks. Chloride-induced stress corrosion cracking (CISCC) of these canisters may occur due to the deliquescence of sea-salt aerosols as the canisters cool. Current experimental and modeling efforts to evaluate canister CISCC assume that the deliquescent brines, once formed, persist on the metal surface, without changing chemical or physical properties. Here we present data that show that magnesium chloride rich-brines, which form first as the canisters cool and sea-salts deliquesce, are not stable at elevated temperatures, degassing HCl and converting to solid carbonates and hydroxychloride phases, thus limiting conditions for corrosion. Moreover, once pitting corrosion begins on the metal surface, oxygen reduction in the cathode region surrounding the pits produces hydroxide ions, increasing the pH under some experimental conditions, leads to precipitation of magnesium hydroxychloride hydrates. Because magnesium carbonates and hydroxychloride hydrates are less deliquescent than magnesium chloride, precipitation of these compounds causes a reduction in the brine volume on the metal surface, potentially limiting the extent of corrosion. If taken to completion, such reactions may lead to brine dry-out, and cessation of corrosion.*

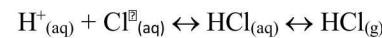
### I. INTRODUCTION

In most published experimental studies of atmospheric corrosion due to sea-salt aerosols, the experimental results are interpreted with the assumption that the salts deposited on the metal surface are sea-salts in composition, and the brines that form *via* deliquescence do not change with exposure time, even after corrosion begins to occur. This is incorrect; once deliquescence occurs, exchange reactions with the atmosphere and corrosion reactions occur, modifying the composition of the salts and brines. Understanding these processes is important because these reactions affect salt and brine compositions, potentially limiting conditions under which corrosion can initiate, or once corrosion begins, limiting the extent of corrosion. Several of these reactions are

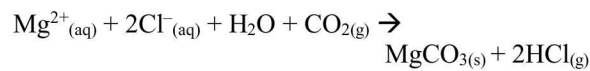
acidification reactions in which acid gases such as HNO<sub>3</sub>, H<sub>2</sub>SO<sub>4</sub> (or SO<sub>2</sub>, which reacts with water to form H<sub>2</sub>SO<sub>4</sub>), or CO<sub>2</sub> (which forms carbonic acid in solution) are absorbed, and concomitant degassing of HCl occurs. This results in conversion of chloride salts to nitrates, sulfates, or carbonates. We have begun evaluating these reactions, focusing on the stability of magnesium chloride brines, which form first as the canister cools and the surface relative humidity (RH) rises, and deposited sea-salt aerosols deliquesce.

### II. MAGNESIUM CHLORIDE BRINE STABILITY

Chloride-containing brines generate a HCl gas partial pressure ( $P_{\text{HCl}}$ ) that is a function of the brine pH and chloride (Cl<sup>-</sup>) concentration:



These brines will degas HCl when the  $P_{\text{HCl}}$  generated by the brine is greater than the atmospheric  $P_{\text{HCl}}$ . When HCl(g) is degassed, the brine pH rises, causing the brine  $P_{\text{HCl}}$  to decrease. In the absence of buffering reactions, degassing is self-limiting—the pH rises until the brine  $P_{\text{HCl}}$  is equal to that in the atmosphere, and then the brine can persist stably. However, degassing can continue if buffering reactions occur, such as acid gas absorption to offset the loss of HCl. In this study, we evaluate the effects of HCl degassing combined with CO<sub>2</sub> absorption. The pH is partially buffered by absorption of CO<sub>2</sub> from the atmosphere and formation of carbonic acid. The carbonate concentration in the brine increases as HCl degassing continues and the pH increases. The brine eventually saturates with a magnesium carbonate phase, which precipitates out. At this point, the pH is fully buffered, and the brine composition becomes invariant; further degassing continues without affecting the pH or the  $P_{\text{HCl}}$ ; the brine can fully convert to the carbonate solid, via:



For simplicity, magnesite ( $\text{MgCO}_3$ ) is shown above, but magnesite itself is kinetically inhibited from precipitating under most conditions<sup>1-3</sup>, and hydromagnesite,  $\text{Mg}_5(\text{CO}_3)_4(\text{OH})_2 \cdot 4\text{H}_2\text{O}$ , is frequently observed experimentally.

Once carbonate precipitation begins, further HCl degassing has no effect on the brine composition, but results in conversion of  $\text{MgCl}_2$  to carbonate and dry-out of the brine. The pH at which this occurs, and the resulting brine  $P_{\text{HCl}}$ , depend upon the identity of the precipitated carbonate phase. To evaluate this thermodynamically, the thermodynamic solubility and speciation modeling program EQ3/6 [Ref. 4] and the Yucca Mountain Program Pitzer database<sup>5</sup> were used. We assume that HCl degassing can occur as soon as the salts deliquesce (or even before, if a water film forms on the salt surface below the deliquescence RH); therefore  $\text{Mg}^{2+}$  and  $\text{Cl}^-$  concentrations were fixed to be at saturation with  $\text{MgCl}_2 \cdot 6\text{H}_2\text{O}$  (bischofite) at each temperature evaluated. This also determines the  $\text{H}_2\text{O}$  activity in the brine. The  $\text{CO}_2$  gas concentration was set to the current atmospheric value of  $10^{-3.4}$  bars. The brine  $P_{\text{HCl(g)}}$  is strongly controlled by the temperature. Therefore, Mg-carbonate and bischofite stability fields were determined as a function of canister surface temperature and atmospheric  $\text{HCl(g)}$  concentration. The results are shown in Figure 1; also shown are typical ranges for atmospheric HCl concentrations in marine, continental, and industrial settings.<sup>6-10</sup>

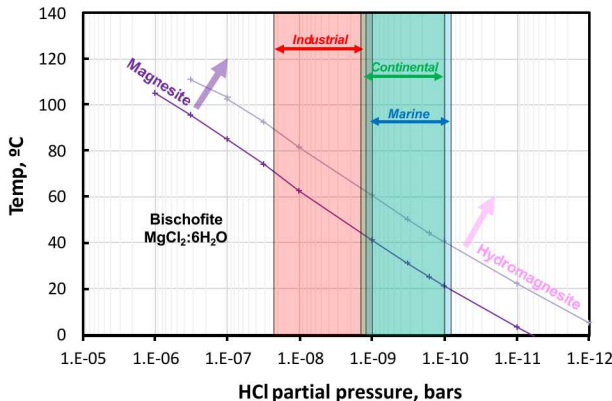


Fig. 1. Stability fields for bischofite, magnesite, and hydromagnesite, as a function of temperature and HCl partial pressure. Atmospheric  $\text{P}_{\text{CO}_2}$  fixed at  $10^{-3.4}$  bars.

At low temperatures, bischofite is the solid stable phase. At elevated temperatures, Mg-Cl brine  $P_{\text{HCl}}$  values are higher, supporting degassing and formation of Mg-carbonate. Stability fields are shown in Figure 1 both for magnesite and for hydromagnesite. Because hydromagnesite is more soluble, it does not precipitate until the pH has risen to a higher value, corresponding to

a lower acid gas concentration—that is why the hydromagnesite stability field is shifted to lower  $\text{HCl(g)}$  values relative to the magnesite field. It is not clear, in concentrated  $\text{MgCl}_2$  brines with low water activities, if magnesite or hydromagnesite would precipitate. While magnesite is generally kinetically inhibited from precipitating, formation under cyclically-varying experimental conditions, which could be relevant to daily temperature and RH fluctuations on a dry storage canister surface, has been observed<sup>2</sup>. Moreover, there are several other known Mg-carbonate minerals with varying numbers of waters of hydration and varying carbonate to hydroxide ratios, and even a Mg-carbonate-chloride phase; most of which are not in the thermodynamic database and cannot be evaluated.

In addition, it is important to note that at the phase boundary conditions, the brine  $P_{\text{HCl}}$  is very low at relevant temperatures. For instance, if magnesite is the solubility-limiting carbonate, then at 60°C, the  $P_{\text{HCl(g)}}$  would be about  $1 \times 10^{-8}$  bars, corresponding to a concentration in the atmosphere about 14  $\mu\text{g}/\text{m}^3$ . In contrast, if hydromagnesite is the precipitating phase, the  $P_{\text{HCl}}$  is an order of magnitude lower, corresponding to 1.3  $\mu\text{g}/\text{m}^3$ . These low capacities for chloride removal may limit the extent of degassing in laboratory settings where air flow rates are low. Estimated air flow rates through interim storage canister overpacks are on the order of cubic meters per minute, and degassing should not be limited by air carrying capacity. However, the rate of HCl loss from the brine surface is also not known and may be kinetically limiting.

## II.A. Testing at 48°C and 40%RH

Given the incomplete thermodynamic data and the potential for kinetic limitations on degassing, the occurrence and rate of this reaction was evaluated experimentally. To do this, magnesium chloride brine (1M, in 17% by volume ethanol solution) was sprayed onto an inert substrate—polished silicon wafers 25 mm in diameter—using an ink-jet printer as described in Schindelholz and Kelly.<sup>11</sup> This deposition method produced randomly-spaced, isolated droplets of brine, approximately 10 – 30 microns in diameter, on the wafer surface. Using dispersed droplets greatly increases the brine surface area-to-volume ratio and increases the rate of exchange with the gas phase. This method produces relevant samples—the droplets are only slightly larger than sea-salt aggregates collected from in-use storage canisters at the Diablo Canyon Independent Spent Fuel Storage Installation,<sup>12</sup> which were ~10  $\mu\text{m}$  in diameter. Initial salt loads were about 37  $\mu\text{g}/\text{cm}^2$   $\text{MgCl}_2 \cdot 6\text{H}_2\text{O}$ . After salt deposition, three samples were retained to quantify the initial condition, and the remaining six samples were placed in a controlled-humidity chamber at

48° C and 40% RH, slightly above the deliquescence RH of  $\text{MgCl}_2 \cdot 6\text{H}_2\text{O}$  (about 35% at that temperature). These conditions are near the maximum temperature at which sea salts are expected to deliquesce under field conditions. The atmosphere in the chamber was replaced at a rate of 2 L/min, using air that had been passed through a “Zero Air” system capable of removing all contaminants (organic compounds and acid gases) from the air stream. The system does not remove  $\text{CO}_2$ . Three samples were pulled after 30 days, and the final three after 69 days. All samples were stored in a cabinet purged with dry nitrogen until analysis.

Once removed from the RH chamber, the samples were examined by scanning electron microscopy/energy dispersive spectroscopy (SEM/EDS). The results indicated that the magnesium chloride had partially converted to magnesium carbonate (Figure 2). Only some of the deposited droplets converted, and even they were not fully converted. The converted droplets exhibited a different morphology, reduced chloride concentrations, and enrichments in carbon (Figure 2). Smaller droplets (<10 $\mu\text{m}$  in diameter) preferentially reacted, possibly because of higher surface-area-to-volume ratios.

Following SEM analysis, the salts were washed off the silicon wafers and analyzed by ion chromatography (IC). The degree of degassing varied, and low salt loads made accurate chemical analysis difficult. The percent chloride lost for the two 69-day samples, was 5% to 7% (Figure 3). At the test conditions, only partial conversion was anticipated. At the  $P_{\text{HCl}}$  predicted by the thermodynamic calculations (Figure 1), each cubic meter of air passing through the humidity chamber could only remove  $\sim 0.4 \mu\text{g}$  (hydromagnesite-buffered) to  $\sim 3 \mu\text{g}$  (magnesite-buffered) of chloride, assuming complete equilibration between brine and atmosphere. At the gas flow rate used (2 L/min) and the measured salt loadings (65.6  $\mu\text{g}/\text{sample}$ ), a single sample would take 15 days (magnesite) to 112 days (hydromagnesite) to lose all chloride. With six samples in the chamber for the first 30 days and three samples for the next 38 days, full degassing was not possible, even if complete equilibration between the headspace gas and the deposited samples had occurred. No such limitation is present for magnesium chloride on a canister surface, because airflow through overpacks is on the order of cubic meters per minute, based on computational fluid dynamics calculations of heat-driven advection through the systems.<sup>9</sup>

These experiments illustrate that HCl degassing does occur from  $\text{MgCl}_2$  brines under conditions relevant to SNF storage, and does result in chloride loss, carbonation, and potentially, brine dryout.

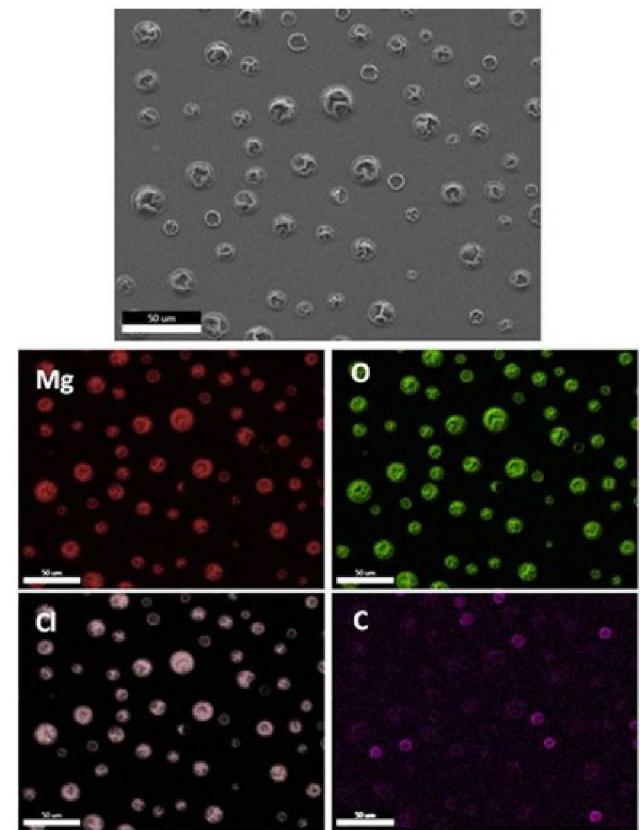


Fig. 2. SEM image and element map of dried magnesium chloride brine droplets exposed for 69 days at 48°C and 40%RH.

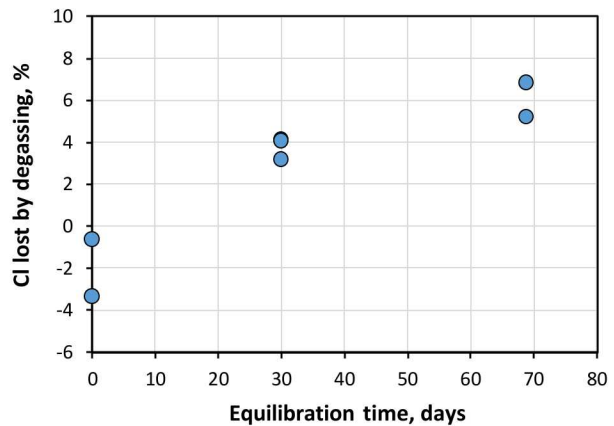


Fig. 3. Fraction of chloride lost, as a function of equilibration time. All measured data are shown, allowing an assessment of experimental uncertainty.

## II.B. Testing at 80°C and 35%RH

Atmospheric corrosion testing is frequently carried out under “accelerated” conditions, combinations of elevated temperatures and RH values that can not be achieved on canisters at the storage sites. These conditions are especially susceptible to acid degassing because higher temperatures result in brines generating higher  $P_{\text{HCl}}$ , leading to higher degassing rates. One such set of conditions, 80°C and 35% RH, is currently being used, and has previously been used,<sup>14</sup> in experimental investigations of SNF storage canister corrosion. Assessing magnesium chloride brine stability is critical to interpreting the result of both the previous and the current experiments.

Under these conditions, the  $P_{\text{HCl}}$  over a magnesium chloride brine in equilibrium with magnesium carbonate is equivalent to 11  $\mu\text{g}/\text{m}^3$  (hydromagnesite) and 83  $\mu\text{g}/\text{m}^3$  (magnesite), potentially resulting in more rapid conversion to carbonate. The experimental design was largely the same as that described above, and the magnesium chloride brine was deposited in the same manner, but a much higher salt load was used to make chemical quantification easier. As a result, droplet coalescence led to a much larger droplet size range than in the previous experiment. Droplets varied from 10 to 150 microns in diameter. The initial salt load was nominally 300  $\mu\text{g}/\text{cm}^2$   $\text{MgCl}_2 \cdot 6\text{H}_2\text{O}$ . After salt deposition, three samples were retained to quantify the initial condition, and the remaining nine samples were placed in a controlled-humidity chamber at 80° C and 35% RH, slightly above the deliquescence RH of  $\text{MgCl}_2 \cdot 6\text{H}_2\text{O}$ . The atmosphere in the chamber was replaced at a rate of 2 L/min, using air that had been passed through the “Zero-air” system described previously. Sets of three samples were pulled, after 14, 28, and 56 days.

Following exposure in the RH chamber, the samples were analyzed in several ways. Selected samples from each sampling time were analyzed by SEM/EDS, and the 56-day samples were analyzed by X-ray diffraction (XRD). Analysis of samples by micro-Fourier Transform Infrared (FTIR) Spectroscopy, micro-Raman spectroscopy, and Time-of-Flight Secondary Ion Mass Spectrometry (TOF-SIMS) are in progress and will provide mineralogical and compositional data. Finally, all samples will be leached with deionized water, and the dissolved salts will be analyzed by IC. IC does not provide information on carbonate, but does give  $\text{Mg}^{2+}$  and  $\text{Cl}^-$  concentrations, allowing estimation of the degree of chloride loss by degassing.

SEM/EDS analysis of representative samples for each exposure time showed major changes in texture and composition over the course of the experiment. After two

weeks, many of the smaller droplets appeared to have lost most of their volume and developed into highly porous masses of fibrous, hairlike crystals. Conversely, the larger droplets mostly retaining a smooth hemispherical outer surface, although some developed a fine hairlike coating, similar to the texture of the smaller droplets. The differences in texture suggest potential variations in mineralogy; however, EDS analysis showed little difference in composition, although the smallest droplets showed a slight decrease in the ratio of Mg:Cl peak areas.

After four weeks, the proportion of small droplets that had developed the fibrous texture had increased, and those that did developed a significantly higher Mg:Cl peak area ratio. Moreover, the droplets showed significant difference in contrast—the droplets exhibiting a higher Mg:Cl ratio appearing darker in backscattered electron images, indicating a lower average atomic number ( $z$ ). As Cl has the highest mass of the elements present, this suggests that the smaller droplets are depleted in  $\text{Cl}^-$ , consistent with the observed changes in Mg:Cl peak area ratios. These results suggest preferential  $\text{Cl}^-$  degassing from the smaller droplets and are consistent with what was observed in the carbonation experiments—smaller droplets with higher surface area-to-mass ratios seem to preferentially react. However, no carbonate phase was observed by SEM/EDS, and X-ray fluorescence spectra of the reacted droplets did not exhibit carbon peaks.

All three 8-week samples were examined by SEM/EDS. There was considerable variability between the samples, and even from location to location on each sample, but in all three cases, significant evidence of chloride loss was observed. Figure 5 is a backscattered electron (BSE) image and element maps of a particularly clear region on Sample #14. There is a clear bimodality in the brightness of the droplets, and the element maps show that the brightness corresponds to compositional differences. Virtually all smaller droplets, and some large droplets, are depleted in chloride and relatively enriched in oxygen. The smaller droplets appear to also be slightly enriched in carbon. EDS X-ray spectra of the droplets are shown in Figure 6. The spectra verify that droplet brightness directly corresponds to degree of  $\text{Cl}^-$  depletion and carbonate enrichment, but also shows droplet size alone is not an accurate discriminant of  $\text{Cl}^-$  depletion or carbonate absorption.

Mg/Cl ratios for all EDS analyses of the 2-week, 4-week, and 8-week samples are shown in Figure 7. There is a clear progression over the course of the experiment. Only the smallest droplets show evidence of chloride loss after 2 weeks, but over time, progressively larger droplets show chloride loss and smaller particles show an increasing degree of chloride loss. By 8 weeks, chloride loss leveled

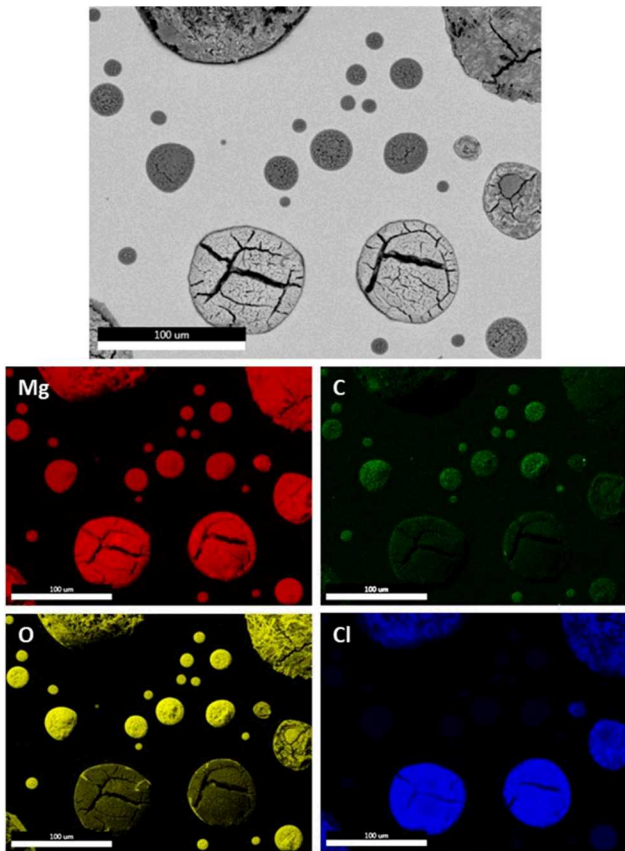


Fig. 5. SEM BSE image and EDS element maps of 8-week  $\text{MgCl}_2$  sample, showing compositional differences with droplet size.

out for the smaller droplets, suggesting that they had completely converted to a different phase.

What phase formed? Although thermodynamic calculations indicate that a magnesium carbonate should form, the amount of carbon present in the 8-week samples is insufficient for the phase to be mostly a carbonate phase. Although thermodynamically favored, it is likely that kinetic limitations, either in carbonate precipitation (magnesium carbonate is notoriously hard to precipitate), or in  $\text{CO}_2$  absorption from the atmosphere, inhibited magnesium carbonate formation. It is likely that kinetic inhibition of carbonate allowed the pH to rise higher in the brine, eventually resulting in precipitation of a magnesium hydroxychloride hydrate, which buffers the pH and allows continued degassing in a manner similar to magnesium carbonate.

Following SEM/EDS analysis, the 8-week samples were characterized by X-ray diffraction (XRD) using a theta/2-theta instrument. Diffraction patterns for two samples (#14 and #19) were dominated by bischofite, but the third sample was inadvertently allowed to deliquesce prior to analysis. This resulted in loss of the bischofite

peaks, and without the interference of bischofite, small peaks of a second phase were observed. These were tentatively identified as a magnesium hydroxychloride hydrate phase with the approximate composition of  $(\text{Mg}(\text{OH})_2)_2\text{MgCl}_2 \cdot 4\text{H}_2\text{O}$ . This phase is generally reported to form in  $\text{Mg}-\text{Cl}$  brines at temperatures above 100°C, however, in at least one study, this phase formed at 80-85°C, similar to the temperature used here.<sup>15</sup> The poor quality of the X-ray diffraction patterns makes the identification tentative; however, the hypothesis is supported by the positive identification of the same phase observed forming by conversion of magnesium chloride brine on the surface of corroding stainless steel under identical test conditions (temperature and RH). This is discussed in the next section. A second important conclusion is that, since the hydroxychloride phase was still present when the bischofite had deliquesced, it must be less deliquescent. If exposed for a sufficiently long time at 80°C and 35% RH, a magnesium chloride brine will eventually convert completely to hydroxychloride and dry out, resulting in cessation of corrosion.

Finally, the 8-week sample showing the greatest degree of reaction was analyzed using micro-Raman spectroscopy and micro-Fourier Transform Infrared (FTIR) Spectroscopy. The micro-Raman patterns for individual droplets varied little and showed minimal structure, although small carbonate peaks were observed in some droplets. However, the FTIR patterns showed major differences with location on the wafer surface, however, the occurrence of sharp hydroxyl bands corresponded with observed areas of high degree of reaction as observed by SEM. Analyses of the FTIR patterns are still in progress, but the data clearly show evidence of phase change associated with sample ageing and HCl degassing. Additional analyses, including TOF-SIMS and chemical analysis, are planned.

### II.C. Magnesium chloride brine stability during metal corrosion

In the previous section, the stability of magnesium chloride brines and salts on an inert substrate was evaluated. This condition potentially applies to magnesium chloride in sea-salts prior to initiation of corrosion. However, once corrosion starts, chemical reactions may result in changes to the brine compositions both in the anode (the pit) and in the surrounding cathode. Anode solutions become highly acidic because of metal hydrolysis reactions, while in the cathode, oxygen reduction results in the generation of hydroxyl groups, and an increase in pH. Several of these reactions could potentially limit the extent of corrosion by removing or sequestering chloride, the corrosive species, or by causing brine dry-out. Acidic conditions in the pit may support acid degassing, potentially resulting in chloride loss from

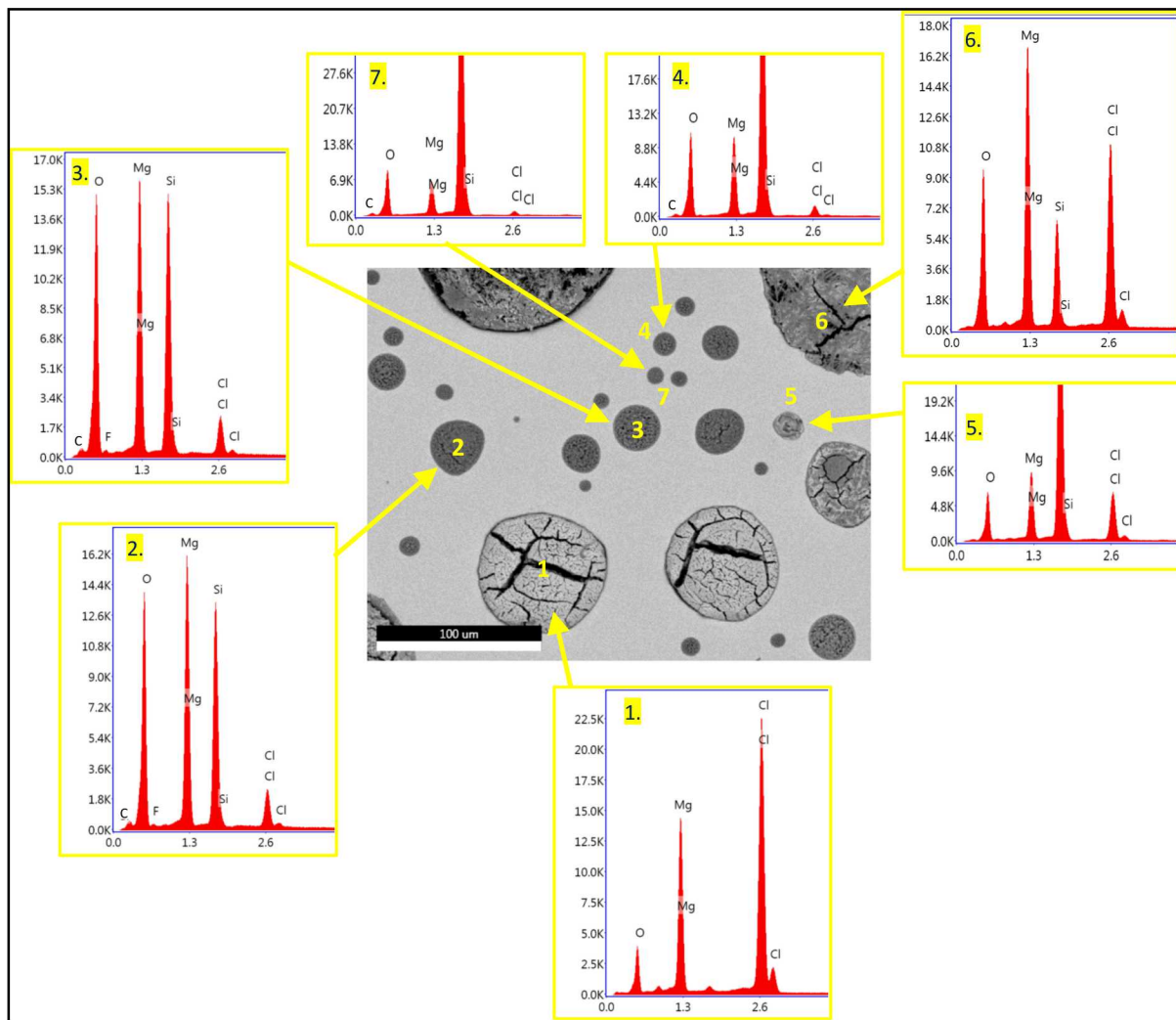


Fig. 6. SEM backscattered electron image and EDS analyses of different droplets, 8-week MgCl<sub>2</sub> sample, showing variations in composition with droplet size and brightness.

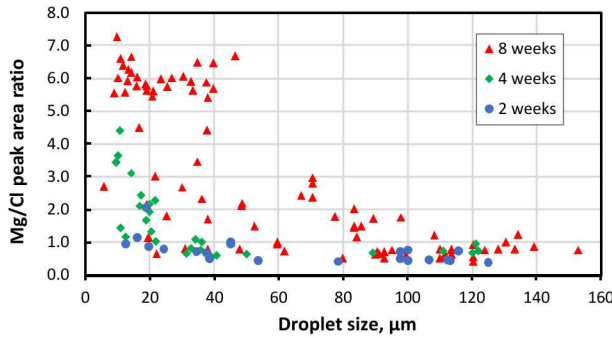


Fig. 7. Comparison Mg/Cl peak area ratios as a function of droplet size, for the 2-week, 4-week, and 8-week  $\text{MgCl}_2$  samples.

the metal surface. As metal ions diffuse away from the pit, the pH increases and hydrolyzed metal ions can precipitate as chloride-containing corrosion products such as akaganeite ( $\text{FeO}(\text{OH},\text{Cl})$ ), sequestering chloride from further reaction. In the cathode, high pH values can cause precipitation of hydroxides, hydroxychlorides, or carbonates (high pH solutions scavenge  $\text{CO}_2$  from the atmosphere), potentially leading to brine dryout.<sup>16</sup>

In experiments with magnesium chloride brines and actively corroding 304 stainless steel, we have observed reactions in the cathode region resulting in precipitation of brine components. In one experiment, droplets of magnesium chloride were deposited a 304 SS 4-point bend specimen, which was then exposed at 80°C and 35% RH, the same conditions as the magnesium chloride brine stability experiment described in Section II.B. After two months in the RH chamber, the sample was heavily corroded. Upon removal from the oven, a white residue was observed surrounding the corroded area (Figure 8, upper). This material was carefully removed from the sample and analyzed by XRD and micro-Raman (Figure 8, lower). The XRD pattern showed that two phases were present, bischofite, and  $(\text{Mg}(\text{OH})_2)_2\text{MgCl}_2 \cdot 4\text{H}_2\text{O}$ , the same phase tentatively identified on the 8-week sample in the magnesium chloride brine stability experiment described in Section II.B. The micro-Raman analysis also showed sharp hydroxyl peaks in the water region ( $3500-3700 \text{ cm}^{-1}$ ) that are not present in bischofite. We conclude that hydroxide generation in the cathodic region resulted in pH rise and precipitation of the magnesium hydroxychloride. This phase is less deliquescent than bischofite (see Section IIB), so sufficient precipitation occurs, the brine will dry out and corrosion will cease.

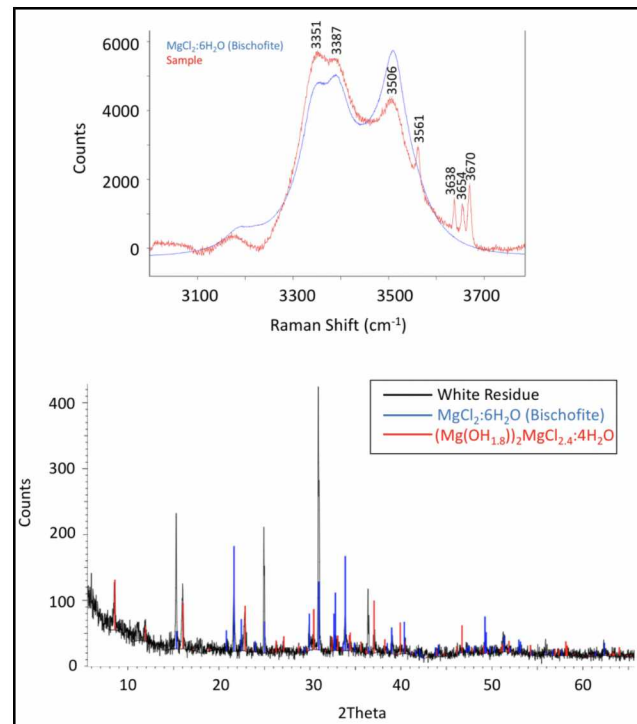
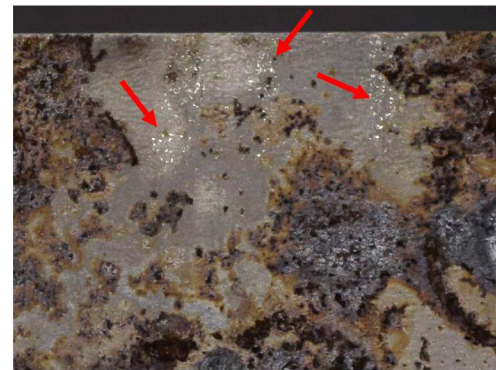


Fig. 8. Upper: white residue (red arrows) surrounding corroded areas on a 304 SS plate coated with magnesium chloride. Lower: X-ray diffraction pattern indicates residue contains a magnesium hydroxychloride, approx.  $\text{Mg}(\text{OH})_2)_2\text{MgCl}_2 \cdot 4\text{H}_2\text{O}$ . Raman-spectrum, shows sharp peaks between  $3500$  and  $3700 \text{ cm}^{-1}$ , confirming the presence of a hydroxyl phase.

### III. CONCLUSIONS

The experimental studies presented here demonstrate that brines formed by sea-salt deliquescence may not persist stably on the heated surfaces of SNF dry storage canisters. Elevated temperatures promote degassing of HCl, a reaction buffered by adsorption of CO<sub>2</sub> from the atmosphere, resulting in conversion of magnesium chloride brines to carbonates. For some conditions, CO<sub>2</sub> absorption may kinetically limit the rate of reaction, allowing conversion to a hydroxychloride phase instead. On a canister surface, these reactions will occur once temperatures drop sufficiently for the sea-salts aerosols to deliquesce. The reactions may occur earlier if adsorbed water films on the un-deliqesced salts, which are known to support corrosion below the deliquescence point, are sufficient to support them. The phases that form are less deliquescent than magnesium chloride, so these reactions may provide additional limits on the temperatures at which corrosion can occur.

Once pitting corrosion begins on the metal surface, metal oxidation is balanced by oxygen reduction in the cathode surrounding the corrosion pits. This reaction produces hydroxide ions, increasing the pH within the cathode region on the metal surface. Under at least some conditions, including the test conditions used here, this leads to precipitation of magnesium hydroxychloride hydrates. Because magnesium carbonates and hydroxychloride hydrates are less deliquescent than magnesium chloride, precipitation of these compounds causes a reduction in the brine volume on the metal surface, potentially limiting the extent of corrosion. If taken to completion, such reactions may lead to brine dry-out, and cessation of corrosion.

Degassing and atmospheric reactions promoted by elevated temperatures must be considered when interpreting the results of laboratory corrosion experiments, especially “accelerated” experiments at elevated temperatures. Ultimately, we hope to include these processes into predictive models for SNF canister corrosion performance in near-marine environments.

### ACKNOWLEDGMENTS

Sandia National Laboratories is a multimission laboratory managed and operated by National Technology and Engineering Solutions of Sandia LLC, a wholly owned subsidiary of Honeywell International Inc. for the U.S. Department of Energy’s National Nuclear Security Administration under contract DE-NA0003525. SAND2019-xxxxxx.

### REFERENCES

1. F. SAYLES and W. FYFE, “The Crystallization of Magnesite from Aqueous Solution,” *Geochimica et Cosmochimica Acta* **37**, 87 (1973).
2. A.P.A. DOA ANJOS, A. SIFEDDINE, C.J. SANDERS, and S.R. PATCHINEELAM, “Synthesis of Magnesite at Low Temperature,” *Carbonates and Evaporites* **26**, 213 (2011).
3. G. MONTES-HERNANDEZ, F. RENARD, R. CHIRIAC, N. FINDLING, and F. TOCHE, “Rapid Precipitation of Magnesite Microcrystals from Mg(OH)<sub>2</sub>-H<sub>2</sub>O-CO<sub>2</sub> Slurry Enhanced by NaOH and a Heat-Aging Step (from ~20° to 90°C),” *Crystal Growth & Design* **12**, 5233 (2012).
4. T.W. WOLERY and R.L. JAREK, *Software User’s Manual, EQ3/6 Version 8.0*, Sandia National Laboratories, Albuquerque, NM (2003).
5. SNL, *In-drift precipitates/salts model, ANL-EBS-MD-000045 REV 03*. Sandia National Laboratories, Albuquerque, NM (2007).
6. B. VIERKORN-RUDOLPH, K. BACHMANN, B. SCHWARZ, and F. MEIXNER, “Vertical Profiles of Hydrogen Chloride in the Troposphere,” *Journal of Atmospheric Chemistry* **2**, 47 (1984).
7. D. MÖLLER, “The Na/Cl Ratio in Rainwater and the Seasalt Chloride Cycle,” *Tellus B* **42**, 254 (1990).
8. G. HARRIS, D. KEMP, and T. ZENKER, “An Upper Limit on the HCl Near-Surface Mixing Ratio over the Atlantic Measured Using TDLAS,” *Journal of Atmospheric Chemistry* **15**, 327 (1992).
9. M. KULMALA, A. TOIVONEN, T. MATTILA, and P. KORHONEN, “Variations of Cloud Droplet Concentrations and the Optical Properties of Clouds due to Changing Hygroscopicity: A Model Study,” *Journal of Geophysical Research: Atmospheres* **103**, 16183 (1998).
10. T. A. CRISP, B. M. LERNER, E. J. WILLIAMS, P. K. QUINN, T. S. BATES, and T. H. BERTRAM, “Observations of Gas Phase Hydrochloric Acid in the Polluted Marine Boundary Layer,” *Journal of Geophysical Research: Atmospheres* **119**, 6897 (2014).
11. E. SCHINDELHOLZ and R.G. KELLY, Application of Inkjet Printing for Depositing Salt Prior to Atmospheric Corrosion Testing. *Electrochemical and Solid State Letters* **13**, C29 (2010).
12. C. BRYAN and D. ENOS, *Analysis of Dust Samples Collected from Spent Nuclear Fuel Interim Storage Containers at Hope Creek, Delaware, and Diablo Canyon, California, SAND2014-16383*. Sandia National Laboratories, Albuquerque, NM (2014).

13. J.M. CUTA and H.E. ADKINS H. E. (2014). *Preliminary Thermal Modeling of HI-STORM 100 Storage Modules at Diablo Canyon Power Plant ISFSI. FCRD-UFD-2014-000505.* Department of Energy, 56 p. (2014).
14. K. SHIRAI, J. TANI, M. WATURU, H. TAKEDA, and T. SAEGUSA. "SCC Evaluation Test of a Multi-purpose Canister." *Proceedings, 13th International High-Level Radioactive Waste Management Conference*, Albuquerque, NM, 10-14 April, 824, American Nuclear Society (2011).
15. J. DE BAKKER, J. LAMARRE, J. PEACEY, and B. DAVIS, "The Phase Stabilities of Magnesium Hydroxychlorides," *Metallurgical and Materials Transactions B* **43**, 758 (2012).
16. R.F. SCHALLER, C.F. JOVE-COLON, J.M. TAYLOR, and E.J. SCHINDELHOLZ, "The Controlling Role of Sodium and Carbonate on the Atmospheric Corrosion Rate of Aluminum," *npj Materials Degradation* **1**, 20 (2017).